Hum Mol Genet. Author manuscript; available in PMC 2013 October 15.

Published in final edited form as:
Hum Mol Genet. 2013 June 15; 22(12): 2482–2494. doi:10.1093/hmg/ddt100.

Pathogenic *NPHP5* mutations impair protein interaction with Cep290, a prerequisite for ciliogenesis

Marine Barbelanne[1,2], **Jenny Song**[1], **Mustafa Ahmadzai**[1], and **William Y. Tsang**[1,2,3,*]

[1]Institut de recherches cliniques de Montréal, 110 avenue des Pins Ouest, Montréal, Québec H2W 1R7, Canada

[2]Faculté de Médecine, Université de Montréal, Montréal, Québec H3C 3J7, Canada

[3]Division of Experimental Medicine, McGill University, Montréal, Québec H3A 1A3, Canada

Abstract

Mutations in the human *NPHP5* gene cause retinal and renal disease but the precise mechanisms by which NPHP5 functions are not understood. We report that NPHP5 is a centriolar protein whose depletion inhibits an early step of ciliogenesis, a phenotype reminiscent of Cep290 loss and contrary to IFT88 loss. Functional dissection of NPHP5 interactions with Cep290 and CaM reveals a requirement of the former for ciliogenesis, while the latter prevents NPHP5 self-aggregation. Disease-causing mutations lead to truncated products unable to bind Cep290 and localize to centrosomes, thereby compromising cilia formation. In contrast, a modifier mutation cripples CaM-binding but has no overt effect on ciliogenesis. Drugs that antagonize negative regulators of the ciliogenic pathway can rescue ciliogenesis in cells depleted of NPHP5, with response profiles similar to those of Cep290- but not IFT88-depleted cells. Our results uncover the underlying molecular basis of disease and provide novel insights into mitigating NPHP5 deficiency.

Introduction

Located in close proximity to the nucleus as a non-membrane bound organelle, the centrosome is the principal microtubule-organizing center critical for cell division in most eukaryotic cells (1, 2). A single centrosome, consisting of a pair of centrioles (termed the mother and daughter centrioles) surrounded by a pericentriolar matrix duplicates in S phase. The duplicated centrosomes migrate to opposite poles of a cell and establish the mitotic spindle at the onset of mitosis, ensuring faithful segregation of chromosomes into daughter cells. Upon cell cycle exit, centrosomes in many cell types template the formation of primary cilia, cellular antennae that sense a wide variety of signals important for growth, development and differentiation (3). Cilia biogenesis or ciliogenesis can be arbitrarily divided into discrete steps (4, 5). First, membrane vesicles carrying protein and lipid cargos are formed at, and recruited to, the distal end of the mother centriole. The centrosome then

*To whom correspondence should be addressed: william.tsang@ircm.qc.ca, Phone: 1 (514) 987-5719, Fax: 1 (514) 987-5685.

Conflict of Interest
The authors have no conflicts of interest to declare.

migrates to the cell cortex, wherein the mother centriole, now transformed into a basal body, attaches itself to the cell membrane and nucleates the formation of an axoneme, the skeleton of a cilium. Docking and fusion of membrane vesicles with the cell membrane also occur simultaneously. The final step of ciliogenesis, intraflagellar transport (IFT) mediates bi-directional transport of cargos and is necessary for cilia biogenesis, function and maintenance. Defects in ciliogenesis can give rise to a bewildering array of human ciliary diseases collectively known as ciliopathies (6, 7). Ciliopathies are pleiotropic and exhibit variable clinical manifestations such as kidney cyst formation, hepatic dysfunction, retinal degeneration and neurological disorders. Although mutations in a number of genes encoding centrosomal and ciliary components are responsible for nearly all ciliopathy cases, the etiology and molecular basis of these diseases remain incompletely understood.

We and others have previously characterized one centrosomal protein, Cep290, whose deficiency is implicated in ciliopathies including Leber congenital amaurosis (LCA; an inherited eye disease characterized by severe loss of vision), Senior-Løken syndrome (SLS; an inherited disorder associated with retinal (severe loss of vision) and renal failure (kidney cyst formation and end-stage renal disease)), nephronophthisis, Joubert syndrome, Bardet-Biedl syndrome and Meckel-Gruber syndrome (8–10). Cep290 participates in primary cilia formation and functions at an early step of the ciliogenic pathway, affecting centrosomal migration and/or anchoring to the cell cortex (11–13). Interestingly, it biochemically interacts with a multitude of proteins, including CP110, a centrosomal protein known to suppress ciliogenesis (12, 14). Identification and characterization of key proteins that associate with Cep290 would greatly enhance our understanding of its roles in ciliogenesis and disease development.

Converging evidence suggests that Cep290 has functional connections with a partially characterized centrosomal/ciliary protein called nephrocystin-5 (NPHP5). First, patients with *NPHP5* mutations exhibit clinical phenotypes that overlap with patients bearing *Cep290* mutations. *NPHP5* mutations constitute a frequent cause of SLS (15, 16). Certain mutations of *NPHP5*, in addition to several SLS-causing mutations, are also detected in patients with LCA, although these patients are believed to be at high risk of developing late-onset renal failure (17, 18). Second, Cep290 is shown to interact with NPHP5 under certain circumstances and therefore the significance of this interaction remains controversial (19–21). Third, ablation of NPHP5 with anti-sense morpholinos in zebrafish leads to the formation of pronephric cysts and phenocopies Cep290 depletion (19). NPHP5 is highly conserved in higher eukaryotes and possesses a putative coiled-coil and IQ calmodulin (CaM)-binding motifs of unknown function (15, 22). Here, we show that NPHP5 localizes to the distal region of centrioles during interphase and is specifically required for early cilia assembly, a function similar to Cep290 but different from IFT88, a protein participating in IFT at a later step of ciliogenesis. Endogenous NPHP5 interacts with Cep290 and CaM, and detailed domain-mapping studies on NPHP5 reveal three separable and functionally distinct domains, namely, the Cep290-binding domain, the CaM-binding domain and the centrosomal localization domain which encompasses the coiled-coil motif. NPHP5 interaction with Cep290 is strictly required for ciliogenesis, while the association between NPHP5 and CaM is needed to prevent NPHP5 self-aggregation. Pathogenic *NPHP5* mutations known to cause SLS and LCA result in the production of truncated products that

are incompetent to bind Cep290 and are mis-localized, thus compromising cilia formation. On the contrary, a *NPHP5* modifier mutation associated with patients with severe retinitis pigmentosa caused by X-linked retinitis pigmentosa GTP regulator (RPGR) deficiency specifically impairs CaM-binding and has no adverse effect on cilia biogenesis. Loss of cilia in the absence of NPHP5 can be rescued by pharmacologically inhibiting negative regulators of ciliogenesis downstream of NPHP5. Interestingly, the response profiles of NPHP5-depleted cells towards different drugs are comparable to those of Cep290- but not IFT88-depleted cells, further suggesting that NPHP5 and Cep290 participate in a common step of the ciliogenic pathway. Cilia formation in cells expressing disease-causing mutants of NPHP5 and treated with drugs can likewise be rescued. Thus, we have uncovered the functional significance of NPHP5 and its interactions with Cep290 and CaM, delineated the molecular mechanisms underlying the pathogenesis of NPHP5-assoicated ciliopathies, and revealed novel pharmacological approaches for treating NPHP5 deficiency.

Results

NPHP5 localizes to the distal region of centrioles and is present in interphase cells

Although NPHP5 is shown to localize to centrosomes and cilia (15, 21, 23), its localization during the cell cycle has not been fully investigated. We used immunofluorescence microscopy to detect NPHP5 localization in diploid human retinal pigment epithelial (RPE-1) cells. This cell line possesses normal centrosome morphology and number and is a well-established model for primary cilia formation. Antibodies against NPHP5 stained two and four prominent spots in G1 and S phase, respectively (Figure 1A). These spots became more diffused in G2 phase and subsequently disappeared in mitosis (Figure 1A). Identical staining patterns were obtained by the use of three antibodies raised against different regions of NPHP5 and also in U2OS cells (data not shown). NPHP5 staining overlapped substantially with that of centrin (Figures 1A and 1B), which is a canonical centriolar protein found at the distal lumen of centrioles. Centrosomal localization of NPHP5 was not affected by treatment with nocodazole (Figure S1A), a microtubule de-polymerizing agent, suggesting that NPHP5 is an intrinsic component of centrosomes. In G0 phase, NPHP5 is present at both the mother centriole/basal body and the daughter centriole, but was never observed along the ciliary axoneme (Figure 1C). Notably, NPHP5 staining at the mother centriole/basal body marginally co-localizes with acetylated and polyglutamylated tubulins in the proximal region, but rather is localized to the distal end near the base of the cilium (Figure 1C).

To further confirm the localization of NPHP5 on centrioles, cells were co-stained with antibodies against NPHP5 and a panel of proximal (C-Nap1, Sas-6 and Flag-Plk4) and distal (CP110, Cep290, Cep164) centriolar markers. NPHP5 showed significant overlap with CP110, Cep290 and Cep164 foci but marginal overlap with dots of Flag-Plk4, C-Nap1 and Sas-6 (Figures 1B and 1D). Thus, our data strongly indicate that NPHP5 is a distal centriolar protein and that it could function during interphase.

NPHP5 depletion inhibits an early step of cilia formation

We examined the consequences of depleting NPHP5 using RNA interference (RNAi)-mediated gene silencing. We transfected either pools of four small interfering RNAs (siRNAs) or five individual siRNAs, and microscopically confirmed the near complete removal of NPHP5 (~90%) from centrosomes in RPE-1 cells (Figures 2A and S1B). Similar observations regarding the loss of NPHP5 signal were made in several non-ciliated (U2OS) and ciliated (ARPE-19 and HEK293) cell lines (Figure S1C), and with the use of three different antibodies against NPHP5 (Figure S1D). To further confirm specificity, Western blot analysis revealed that NPHP5 antibodies recognized one specific band corresponding to a size of ~69kDa, and more importantly, protein levels were elevated in cells over-expressing Flag-NPHP5 and reduced by ~80% in NPHP5 siRNA-treated cells (Figure 2B). Of note, although endogenous NPHP5 was readily detected in HEK293 extracts, it was undetectable in lysates of RPE-1 and U2OS cells (Figure 2B), suggesting that this protein is of low abundance in the latter two cell lines. Next, we determined whether NPHP5 is needed for different aspects of centrosome function. Depletion of NPHP5 did not induce abnormal number of centrin or γ-tubulin foci (Figures S2A–B), abnormal separation of centrin foci (Figure S2C), aberrant mitotic figures (data not shown) or mitotic arrest (Figure S2D), and therefore had no significant impact on centriole/centrosome duplication, centriole/centrosome separation or mitotic division. Further flow cytometric analysis indicated that suppression of NPHP5 did not alter cell cycle progression (Figure S2E).

Given its connection with human ciliopathies, we tested a role for NPHP5 in the assembly of primary cilia. RPE-1 cells were transfected with control or NPHP5 siRNAs, uninduced or induced to quiescence, and stained for ciliary markers including glutamylated tubulin, acetylated tubulin, IFT88 and Gli2. The percentages of ciliated cells are different between proliferative and quiescent states, and hence it is critical to evaluate if NPHP5 perturbs cilia formation under both conditions. Interestingly, ablation of NPHP5 led to a dramatic two-fold reduction in the ability of cells to assemble cilia in cycling and quiescent cells (20% to 10% for cycling and 80% to 40% for quiescent cells; Figure 2C). Similar results were obtained with another retinal pigment epithelial cell line, ARPE-19 (data not shown), and these findings were consistent with a systematic analysis designed to unravel the roles of ciliary disease proteins in cells and tissues (21). The failure to undergo ciliogenesis in NPHP5-depleted cells was not due to cell cycle defects (Figures S2D–E) or an inability of the cell to enter a quiescent state, as revealed by Ki67 staining (Figure 2D). Subsequently, we pinpointed the step(s) at which cilia formation is blocked. Loss of NPHP5 did not impinge on centrosomal accumulation of Rab11a-positive vesicles, suggesting that early vesicular trafficking events, including the formation of pericentrosomal preciliary compartment (24), are not affected (Figures S2F). In light of the *in vivo* interaction between NPHP5 and Cep290 (Figure 3A) and the role of Cep290 in the migration and/or anchoring of centrosomes to the cell cortex during early ciliogenesis, we examined the distance between centrosomes and nuclei in NPHP5-depleted RPE-1 cells. As a control, we performed identical experiments in cells depleted of IFT88, a protein dispensable for centrosome migration but required for a late step of ciliogenesis (25). Strikingly, ~60% of the centrosomes in quiescent control and IFT88-depleted cells were well separated from the nucleus and were localized close to the cell surface, in contrast to ~30% in NPHP5- and

Cep290-depleted cells (Figure 2E). Taken together, depletion of NPHP5, like Cep290, disrupts the migration and/or anchoring of centrioles to the cell cortex and inhibits ciliogenesis.

NPHP5 interaction with Cep290 is critical for ciliogenesis

Despite circumstantial evidence that NPHP5 interacts with Cep290 (19–21), an endogenous interaction between the two proteins has not been demonstrated and its physiological relevance remains unclear. To determine whether endogenous proteins associate *in vivo*, we performed immunoprecipitations with NPHP5 and Cep290 antibodies. NPHP5 and Cep290 were co-immunoprecipitated by NPHP5 antibodies, and reciprocal immunoprecipitations with Cep290 antibodies confirmed a robust physiological interaction (Figure 3A). Next, we generated a series of Flag-tagged Cep290 truncation mutants, performed anti-Flag immunoprecipitations and examined their ability to interact with NPHP5 in cell extracts. We found that the NPHP5-binding domain of Cep290 was mapped between residues 790-816 (Figures S3A-B), consistent with two previous studies showing a requirement of the N-terminal region for binding to NPHP5 (19, 21). In addition, domain-mapping experiments were performed to identify the region of NPHP5 responsible for its interaction with Cep290. A C-terminal region of NPHP5 interacted with Cep290, and further efforts to delete or mutate conserved residues within this region revealed that residues 509-529 and 549 were both critical for binding (Figures 3B–D). Notably, the Cep290- and calmodulin-binding domains of NPHP5 are separable, as mutants with impaired binding to Cep290 could still associate with CaM (Δ509-529 and A549K; Figures 3B and 3D), and vice versa (ΔIQ123; Figures 5A–B). Both domains are also distinct from the centrosomal localization domain which encompasses the coiled-coil motif (residues 340-371) and residue 547 (Δ340-371, Δ543-555 and A547K; Figures 3C–D, 4C and S4). Thus, we have successfully generated small deletions and single amino acid substitutions that specifically cripple Cep290-binding, CaM-binding or protein localization to the centrosome. Finally, Far-Western blot experiments revealed a direct association of NPHP5 with Cep290 (Figure S3C).

To delineate the biological significance of the NPHP5-Cep290 interaction, we performed reciprocal depletion of NPHP5 and Cep290 using RNAi. Ablation of NPHP5 has no effect on the levels or localization of Cep290. However, loss of Cep290 significantly disrupts NPHP5 centrosomal localization without affecting its protein levels (Figures 4A-B). Although these observations led to the speculation that Cep290 recruits NPHP5 to the centrosome (21), we do not believe this is the case. We demonstrated from our large collection of NPHP5 mutants that four mutants proficient in Cep290-binding (Δ340-371, A547K, fragments 419-598 and 287-530) could not be targeted to the centrosome, and conversely, two mutants deficient in Cep290-binding (Δ509-529 and A549K) were properly targeted (Figures 3C-D, 4C and S4). These data argue against a role for Cep290 in recruiting NPHP5 to the centrosome and further reinforce the notion that the Cep290-binding and centrosomal localization domains of NPHP5 are separable.

We then carried out rescue experiments in which wild type or mutant NPHP5 was expressed in quiescent cells depleted of endogenous NPHP5. We note that, whereas wild type was able to rescue ciliogenesis, mis-localized mutants (Δ340-371, Δ543-555 and A547K) failed to do

so irrespective of their Cep290-binding status (Figures 3D and 4D). Most remarkably, mutants that are localized to centrosomes but do not bind Cep290 (Δ509-529 and A549K) also failed to restore cilia formation (Figures 3D and 4D). These results establish a clear and important mechanistic link between NPHP5-binding to Cep290 and ciliogenesis.

NPHP5 interaction with CaM prevents self-aggregation

The foregoing results suggest that the distinct binding domains for Cep290 and CaM in NPHP5 could serve different biological functions. To begin characterizing the interaction between NPHP5 and CaM, we showed that the two proteins associated with each other in the presence or absence of calcium from extracts supplemented with calcium ($+Ca^{2+}$) or EGTA ($-Ca^{2+}$) (Figure S5A). Further, both wild type and mutant CaM refractory to Ca^{2+}-binding (CaM1234) interacted equally well with NPHP5 (Figure S5B), and these results together confirmed a previous report that NPHP5 and CaM interact in a Ca^{2+}-dependent and Ca^{2+}-independent manner (22). Bacterially expressed NPHP5 robustly bound to purified CaM *in vitro*, strongly suggestive of a direct interaction (Figure S5C). The Calmodulin Target Database predicts the existence of three putative IQ motifs in NPHP5 (residues 300-328, 391-410 and 420-437 and denoted IQ1, IQ2 and IQ3, respectively; Figure 3C). Using a series of Flag-tagged NPHP5 truncation and deletion mutants wherein the IQ motifs were removed singly or in combination, we demonstrated that the first and second motifs, IQ1 and IQ2, were most critical for binding to CaM (Figures 3B–C, 5A–B). Complete loss of binding, however, was achieved only when all three IQ motifs were deleted (ΔIQ123; Figures 5A–B). Loss of CaM-binding does not compromise Cep290-binding (Figures 5A–B), strengthening an earlier point that the CaM- and Cep290-binding domains of NPHP5 are separable. In addition, we showed that recombinant GFP-NPHP5 and endogenous CaM co-immunoprecipitated with recombinant Flag-Cep290 (Figures S3A–B), and likewise, endogenous Cep290 and GFP-NPHP5 were detected in Flag-CaM immunoprecipitates (Figure S5B). Moreover, antibodies against NPHP5 and Cep290 co-precipitated endogenous CaM (Figure 3A). Taken together, these data indicate that IQ motifs of NPHP5 mediate CaM-binding and that NPHP5 forms a complex with Cep290 and CaM.

Next, we investigated the functional consequences of the NPHP5-CaM interaction. Unlike mutations that specifically cripple the centrosomal localization or the Cep290-binding domain, the CaM-binding mutant, ΔIQ123 still showed centrosomal targeting and was fully able to rescue cilia formation in NPHP5-depleted cells (Figures 5B–C and S5D). Noticeably, we observed the formation of punctate foci or aggregates in the cytoplasm of mutant cells (Figure 5D and S5D). These cytoplasmic aggregates were devoid of centrosomal markers such as centrin, CP110, γ-tubulin and Cep290 (Figure S5D), suggesting that they do not recruit any centrosomal proteins to extra-centrosomal sites and therefore arise from self-assembly. In addition, aggregate formation is unlikely to be triggered by elevated levels of expression, since the levels of wild type and mutant proteins were comparable (Figure 5A). To further strengthen the correlation between impaired CaM-binding and aggregate formation, we found that removal of the first two IQ motifs (ΔIQ12) or a point mutation in the second IQ motif (I393N) of NPHP5 severely weakened mutant protein interaction with CaM and induced aggregate formation (to a lesser extent compared to ΔIQ123) without affecting protein localization to centrosomes, binding to Cep290, or ciliogenesis (Figures

5A–D and S5D; also see below). In summary, NPHP5 mutants deficient in CaM-binding are aggregation-prone and CaM may serve as a chaperone to protect the mis-folding and aggregation of NPHP5 through direct interaction.

Molecular and functional consequences of *NPHP5* disease mutations

The differential roles of NPHP5 interactions with Cep290 and CaM prompted us to investigate their relevance in human disease. The vast majority of the >15 pathogenic *NPHP5* mutations identified in SLS and LCA patients are compound heterozygous or homozygous non-sense and frameshift mutations. No apparent correlation exists between genotype and phenotype, and the same mutation can often cause LCA and SLS (15–18, 26–28). These mutations are located in the internal regions of the gene and predicted to encode truncated products lacking the C-terminal tail (Figure 6A; (15–18, 26–28)). Since the C-terminal tail contains the centrosomal localization and Cep290-binding domains, loss of Cep290-binding and protein mis-localization could underlie the disease mechanism in patients carrying *NPHP5* mutations. We examined five *NPHP5* mutations (F142fsX146, R332X, R461X, R502X and H506fsX518) commonly found in disease patients, including two at the extreme 5′ and 3′ ends, and tested whether they affect protein expression, localization to centrosomes and interaction with Cep290 and CaM, and cilia formation in rescue experiments. R332X and R502X mutations are detected in patients with SLS and LCA, respectively, while F142fsX146, R461X and H506fsX518 mutations are associated with SLS and LCA (Figure 6A). These mutations resulted in shorter and faster-migrating proteins as expected, and their expression levels were relatively similar to full-length protein (Figure 6B). Interestingly, while two mutants, F142fsX146 and R332X failed to interact with CaM, all were incompetent in binding to Cep290 (Figures 6A and 6B), mis-localized (Figures 6C and S6A) and unable to rescue ciliogenesis (Figures 6D and S6B). Thus, disease-causing mutations of *NPHP5* render the resulting proteins non-functional.

In addition to its pathogenic role in SLS and LCA, *NPHP5* is reported to be a modifier gene for a different retinal disorder, namely, retinitis pigmentosa. In this case, a natural polymorphic variation in *NPHP5*, I393N, strongly associates with disease severity in patients with RPGR deficiency (29), suggesting that it may contribute to the development of disease symptoms. Remarkably, we found that I393N mutation induced only subtle molecular and cellular defects, including diminished protein binding to CaM and increased aggregate formation, but had no effect on protein localization to the centrosome and cilia formation (Figures 5A–D and S5D). These results contrast sharply with those of disease-causing mutations (Figure 6).

Pharmacological rescue of cilia formation in the absence of NPHP5

One prediction stemming from our studies is that since NPHP5 is a positive regulator at an early step of ciliogenesis, modulation of downstream events in the ciliogenic pathway could mitigate or correct the effects of NPHP5 deficiency and restore cilia formation. Several cellular processes, such as removal of a “cap” at the distal end of the mother centriole, focal adhesion disassembly, actin de-polymerization and membrane trafficking are known to be important for ciliogenesis (14, 24, 30, 31). These highly dynamic processes are controlled by a number of negative regulators, including CP110, focal adhesion kinase (FAK), actin-

related protein 3 (ARP3) and secreted phospholipase A2 Group 3 (PLA2G3) (Figure 7A). In addition, X-lined inhibitor of apoptosis (XIAP) also inhibits cilia biogenesis, although its role in centrosome and cilium biology is virtually unknown (Figure 7A; (24)). Given that loss of these proteins facilitate ciliogenesis in cycling cells (14, 24, 30, 31), we tested whether their depletion or inhibition could rescue cilia formation in cells depleted of NPHP5. We first examined the consequences of knocking down NPHP5, CP110, or both by RNAi. Depletion of CP110 led to aberrant formation of cilia (Figure 7B), consistent with our previous observations (12, 14). However, ablation of both NPHP5 and CP110 suppressed the phenotype associated with CP110 depletion and mimicked NPHP5 ablation (Figure 7B), suggesting that CP110 inhibition cannot compensate for the loss of NPHP5. Next, we determined that treatment of control cells with drugs targeting FAK, actin, ARP3, PLA2G3 and XIAP resulted in a two-fold enhancement of cilia formation following dose optimization (Figures 7A and data not shown). Remarkably, certain drugs dramatically rescued the loss of cilia phenotype caused by depletion of NPHP5 (Figures 7C and S7A). PF573228, Cytochalasin D and latruculin B, in particular, restored ciliogenesis to levels comparable to control, whereas FAK inhibitor 14, CK548 and embelin were the least potent (Figure 7C). Of note, drug response profiles of NPHP5-depleted cells were remarkably similar, if not identical, to those of Cep290-depleted cells (Figures 7C and S7A), further suggesting that NPHP5 and Cep290 depletion inhibit a common pathway in cilia assembly. The same set of drugs, however, elicited different responses in cells depleted of IFT88, with FAK Inhibitor 14, cytochalasin D, CK548 and embelin being the most potent in rescuing cilia formation (Figure 7C). PF573228 and latruculin B, in striking contrast, were practically ineffective in IFT88-depleted cells (Figure 7C). Finally, we performed experiments in which we depleted endogenous NPHP5, expressed disease-causing mutants of NPHP5 and subsequently treated cells with cytochalasin D, and found that cilia formation was drastically restored (Figure S7B). Considered together, our findings indicate that ciliary defects associated with deficiencies in NPHP5/Cep290 and IFT88 can be differentially rescued by pharmacological means.

Discussion

Ciliogenesis is a poorly understood dynamic process requiring precise coordination of multiple cellular events and proteins. Elucidating the molecular mechanisms through which these proteins function is crucial to understanding their roles in human ciliopathies. We and others have previously described Cep290, a human ciliary disease protein required for ciliogenesis (11–13). Here, we characterize another ciliopathy protein, NPHP5, and show that the two proteins share a number of common characteristics. First, NPHP5 and Cep290 strictly function at an early step of ciliogenesis and participate in the migration and/or anchoring of centrosomes to the cell cortex. Second, NPHP5 interacts with Cep290 in a physiologically relevant setting and their direct association is necessary for ciliogenesis. Third, drugs that rescue the loss of cilia phenotype associated with NPHP5 depletion are also effective in rescuing the Cep290 depletion phenotype. Despite these similarities, it is also clear that the two proteins differ in several important aspects. Whereas NPHP5 is targeted to centrioles, Cep290 is known to localize to both centrioles and centriolar satellites (11, 20, 32, 33). Furthermore, loss of Cep290 disrupts the localization of a well-known

satellite protein percentriolar material-1 (PCM-1) to satellites, a phenotype we did not observe upon NPHP5 depletion (data not shown). Several satellite proteins, including PCM-1, are essential for cilia biogenesis, underscoring the importance of these peculiar structures in cilium biology (34). In addition, the clinical spectrum of *Cep290* mutations is more diverse compared to that of *NPHP5* mutations, implying that Cep290 could possess additional biological roles and/or function in multiple cell and tissue types. Further studies will be needed to dissect the relative contribution of NPHP5 and Cep290 to ciliogenesis and ciliopathies.

Although we have identified critical functional domains in NPHP5, including the centrosomal localization domain, the molecular mechanisms through which NPHP5 is recruited to the centrosome remain unknown. In light of our findings with NPHP5 mutants and reciprocal depletion of NPHP5 and Cep290, we speculate that targeting of NPHP5 could entail an unidentified factor X. This factor recognizes and binds to the centrosomal localization domain of NPHP5 and transports it to the centrosome. Once there, factor X transiently interacts with a docking platform containing Cep290 wherein it presents NPHP5 to Cep290. Experiments are currently underway to reveal the identity of factor X and to test the validity of our proposed recruitment mechanism.

It is clear from our studies that the differential roles of NPHP5 interactions with Cep290 and CaM have important clinical implications. Disease-causing mutations of *NPHP5* induce two crucial and universal defects, namely protein mis-localization and incompetence in binding Cep290, both of which interfere with cilia assembly. On the other hand, a *NPHP5* modifier mutation identified in patients with RPGR deficiency specifically cripples CaM-binding and causes NPHP5 self-aggregation. Although these aggregates do not appear to affect ciliogenesis, their presence might be detrimental in the long run or under certain pathophysiological conditions. Since it is known that protein aggregation can lead to an accumulation of amyloid fibrils (35), a hallmark of neurodegenerative disorders, it is plausible that NPHP5 aggregates could induce amyloidosis and contribute to the severity of retinitis pigmentosa, a degenerative eye disease. Future experiments aimed at unraveling how this modifier mutation might compromise protein function and/or induce cellular toxicity will greatly enhance our knowledge of disease pathogenesis.

The series of molecular and cellular events leading to cilia formation have not been elucidated. Our work strongly suggests that removal of CP110 “cap” from the distal end of the mother centriole precedes NPHP5-mediated migration and/or anchoring of centrosomes to the cell surface, and a similar relationship between CP110 and Cep290 has previously been documented (12). On the other hand, PF573228 and latrunculin B dramatically rescue cilia formation in NPHP5- and Cep290- but not IFT88-depleted cells, and therefore, actin de-polymerization and focal adhesion disassembly might lie “downstream” of NPHP5 and Cep290 function. Both drugs are highly specific to their targets: latrunculin B is a membrane-permeable compound known to bind monomeric G-actin in the nanomolar range (IC_{50}=10 nM), while PF573228 (IC_{50}=4 nM) is one of the many potent inhibitors of FAK currently being evaluated for potential utility in cancer therapeutics (36, 37). Thus, one intriguing possibility is that NPHP5 and Cep290 directly or indirectly sequester G-actin and/or inactivate FAK, thereby promoting centrosome migration and/or anchoring to the cell

cortex. It will be interesting to determine whether NPHP5 and Cep290 bind to monomeric actin and/or focal adhesion complex, as understanding these mechanisms will provide novel insights into the development of therapeutic strategies for ciliopathies.

Materials and Methods

Cell Culture and Plasmids

Human ARPE-19, U2OS, hTERT RPE-1 and HEK293 cells were grown in DMEM supplemented with 10% FBS at 37°C in a humidified 5% CO2 atmosphere. To generate Flag-tagged NPHP5 fusion proteins, human NPHP5 cDNA fragments encoding residues 1–598 (full-length or FL), 1-157, 168-414, 419-598, 96-279, 287-493, 287-506, 287-530, 287-554, 287-579, 287-598, 336-598 and 380-598 were amplified by PCR using Phusion High-Fidelity DNA Polymerase (New England Biolabs) and sub-cloned into mammalian expression vector pCBF-Flag (gift from B. Dynlacht). The following NPHP5 deletions and point mutations (Δ340-371, Δ509-529, Δ543-555, A547K, K548A, A549K, K550A, Q551A, Δ300-328 (ΔIQ1), Δ391-410 (ΔIQ2), Δ420-437 (ΔIQ3), Δ300-328Δ391-410 (ΔIQ12), Δ300-328Δ420-437 (ΔIQ13), Δ391-410Δ420-437 (ΔIQ23), Δ300-328Δ391-410Δ420-437 (ΔIQ123), I393N, F142fsX146, R332X, R461X, R502X, H506fsX518) were introduced into full-length cDNA by employing a two-step PCR mutagenesis strategy and sub-cloned into pCBF-Flag. Human NPHP5 was also sub-cloned into mammalian vector pEGFP-C1 and bacterial expression vector pET23a (gift from J.F. Cote) to generate GFP-NPHP5 and NPHP5-His, respectively. To generate Flag-CaM and Flag-CaM1234, rat CaM and CaM1234 (gift from J. Adelman) were amplified by PCR and sub-cloned into mammalian vector pFlag-CMV5. To generate Flag-Cep290, Cep290 fragments encoding residues 696-790, 696-822, 696-896, 720-896, 746-896, 762-896, and 780-896 were amplified by PCR and subcloned into pCBF-Flag. All constructs were verified by DNA sequencing. Other Flag-Cep290 constructs were previously described (12). A plasmid DNA expressing Flag-Plk4 was obtained from K. Lee.

Antibodies

Antibodies used in this study included anti-CP110, anti-CEP290 (Bethyl Laboratories), anti-centrin (Millipore), anti-C-Nap-1, anti-Sas-6, anti-NPHP5, anti-Gli2, anti-Rab11a (all from Santa Cruz), anti-PCM-1 (gift from A. Merdes), anti-α-tubulin, anti-acetylated tubulin, anti-Flag, and anti-γ-tubulin (all from Sigma-Aldrich), anti-glutamylated tubulin GT335, anti-Cep170, anti-Ki67 (all from Invitrogen), anti-IFT88, anti-NPHP5 (ProteinTech), anti-Cep164 (gift from E. Nigg), anti-CaM and anti-NPHP5 (Abcam). To generate rabbit anti-NPHP5 antibodies, a glutathione-S-transferase (GST) fusion protein containing residues 1-131 (IRCM2) and 469-598 (IRCM1) of NPHP5 was expressed in *E. coli* and purified to homogeneity. Antibodies against NPHP5 were purified by affinity chromatography.

Immunoprecipitation, Immunoblotting, and Immunofluorescence Microscopy

Cells were lysed with buffer (50 mM HEPES/pH 7, 250 mM NaCl, 5 mM EDTA/pH 8, 0.1% NP-40, 1 mM DTT, 0.5 mM PMSF, 2 μg/ml leupeptin, 2 μg aprotinin, 10 mM NaF, 50 mM β-glycerophosphate and 10% glycerol) at 4°C for 30 min and extracted proteins were recovered in the supernatant after centrifugation at 16,000g. In experiments involving

calcium, 2.5 mM CaCl2 (+Ca2+) or 5 mM EGTA (−Ca2+) was also added to the lysis buffer. After centrifugation, 2 mg of the resulting supernatant was incubated with an appropriate antibody at 4oC for 2 hours and collected using protein A Sepharose. The resin was washed with lysis buffer, and bound proteins were analyzed by SDS-PAGE and immunoblotting using appropriate primary antibodies and horseradish peroxidase (HRP)-conjugated secondary antibodies (VWR). Typically, 50–150 μg of lysate was loaded into the input (IN) lane. For mapping studies, Flag-tagged constructs alone or in combination with GFP-tagged constructs were transfected into HEK293 cells. Cells were harvested 48–72 hr after transfection. Anti-Flag M2 beads (Sigma-Aldrich) were used for immunoprecipitations. For indirect immunofluorescence, cells were grown on glass coverslips, fixed with cold methanol or 4% paraformaldehyde and permeabilized with 1% Triton X-100/PBS. Slides were blocked with 3% BSA in 0.1% Triton X-100/PBS prior to incubation with primary antibodies. Secondary antibodies used were Cy3-, Cy5- or Alexa488- conjugated donkey anti-mouse, anti-rat or anti-rabbit IgG (Jackson Immunolabs and Molecular Probes). Cells were then stained with DAPI, and slides were mounted, observed, and photographed using a Leitz DMRB (Leica) microscope (100×, NA 1.3) equipped with a Retiga EXi cooled camera. For analysis of the distance between the centrosome and the nucleus, z-sections spaced by 0.2μm were taken using a DM6000 B (Leica) microscope (100×, NA 1.4) equipped with a Hamamatsu Orca-ER camera (model C-4742). The xyz coordinates of the centrosome and the center of the nucleus were determined using Volocity6 (PerkinElmer) and distance was calculated using the formula $d=\sqrt{(x_2-x_1)^2+(y_2-y_1)^2+(z_2-z_1)^2}$. When the distance between the centrosome and the nucleus was >7μm, the centrosome was considered to be migrated to the cell surface. A distance of <7μm signified no migration.

Pharmacological Studies

Cells were treated with varying concentrations of cytochalasin D, CK636, CK548 (Sigma), TPEN, CAY10590, OPC, latrunculin B (Cayman Chemical), embelin, PF573228 or FAK Inhibitor 14 (Tocris Bioscience) and incubated for 8h before fixation. For each drug, the concentration required to induce maximal ciliated cell numbers with minimal toxicity was determined and used in subsequent experiments. As a vehicle control, an equivalent amount of DMSO or ethanol was added, and neither has an effect on cilia formation.

RNA Interference

Synthetic siRNA oligonucleotides were purchased from Dharmacon. Transfection of siRNAs was performed using siImporter (Millipore) per manufacturer's instructions. The 21-nucleotide siRNA sequence for the nonspecific control (NS) and IFT88 were 5-AATTCTCCGAACGTGTCACGT-3′ and 5′-CCGAAGCACTTAACACTTATT-3′, respectively. The 21-nucleotide siRNA sequences for NPHP5 were: 5′-GAGCAGAATGTCCCTGTTA-3′ (oligo 1), 5′-ACCCAAGGATCTTATCTAT-3′ (oligo 2), 5′ GAGGCCATGTTGAACTTAT-3′ (oligo 3), 5′-CCAAATAGGATCTGCAGTC-5′ (oligo 4) and 5′-CCCTAAGAATTGACACAAA-3′ (oligo 5). siRNA oligo 2 was used to deplete endogenous NPHP5 unless otherwise stated. siRNA oligo 5, which targets the 3′UTR of NPHP5 mRNA, was used to deplete endogenous NPHP5 in cilia rescue experiments. The siRNAs for Cep290 and CP110 silencing were previously described (12).

Induction of Primary Cilia

RPE-1 or ARPE-19 cells transfected with siRNA were brought to quiescence by serum starvation for 48–72 hr. Cells were examined for well-established primary cilium markers such as acetylated tubulin, glutamylated tubulin, IFT88 or Gli2.

Cell Cycle Synchronization and Fluorescence-Activated Cell Sorting Analysis

Cells were fixed in 95% ethanol at 4°C for at least 1 hr and were subsequently incubated with 0.1 mg/ml RNase A in PBS at 37°C for 30 min. After centrifugation and removal of supernatant, cells were stained with 50 ug/ml propidium iodide at 4°C for 30 min. Samples of 100,000 cells were analyzed with a FACScalibur flow cytometer and CellQuest and FlowJo cell cycle analysis software.

Far Western Blotting and *In Vitro* Binding Assay

For Far Western blotting, membrane was incubated in AC buffer (0.1 M NaCl, 20 mM Tris/pH 7.5, 1 mM EDTA/pH 8, 0.05% Tween 20, 3% milk, 1 mM DTT, 10% glycerol) containing 6 M guanidine-HCl for 30 min at 22°C, followed by AC buffer with 3 M guanidine-HCl for 30 min. at 22°C, AC buffer with 0.1 M guanidine-HCl for 30 min. at 4°C, and AC buffer only for 1 hr at 4°C. After blocking with 3% milk for 1 h at 22°C, membrane was incubated with purified GST-NPHP5(469-598) bait protein in binding buffer (0.1 M NaCl, 20 mM Tris/pH 7.5, 0.5 mM EDTA/pH 8, 0.1% Tween 20, 3% milk, 1mM DTT, 10% glycerol) overnight at 4°C. Bait protein was detected by anti-GST conjugated to HRP (GenScript). For *in vitro* binding, bacterially purified NPHP5-His mixed with purified GST or calmodulin (Cedarlane) at 4°C for 1h was incubated with HisPur cobalt resin (Thermo Scientific) at 4°C for another hour. After extensive washing with equilibration buffer (50mM $NaPO_4$, 300mM NaCl, 10mM imidazole/pH 7.4), bound proteins were analyzed by SDS-PAGE and immunoblotting.

Statistical Analysis

The statistical significance of the difference between two means was determined by using a two-tailed Student's *t* test. Briefly, the means and standard deviations of two data sets were determined in order to generate a *t* value. The *t* value was used in conjunction with the degrees of freedom to obtain a *p* value. Differences were considered significant when $p<0.01$.

Supplementary Material

Refer to Web version on PubMed Central for supplementary material.

Acknowledgments

We thank all members of the Tsang laboratory for constructive advice. We thank N. Al-Bader and H. Ling for assistance with cloning and anti-NPHP5 antibody generation, respectively. We thank E. Nigg and A. Merdes for providing antibodies, and K. Lee, J. Adelman, J.F. Cote and B. Dynlacht for providing plasmids. W.Y.T. was a Canadian Institutes of Health Research New Investigator and a Fonds de recherche Santé Junior 1 Research Scholar. This work was supported by the Canadian Institutes of Health Research (IC1-111427 and MOP-115033 to W.Y.T.).

References

1. Brito DA, Gouveia SM, Bettencourt-Dias M. Deconstructing the centriole: structure and number control. Curr Opin Cell Biol. 2012; 24:4–13. [PubMed: 22321829]
2. Nigg EA, Stearns T. The centrosome cycle: Centriole biogenesis, duplication and inherent asymmetries. Nat Cell Biol. 2011; 13:1154–1160. [PubMed: 21968988]
3. Ishikawa H, Marshall WF. Ciliogenesis: building the cell's antenna. Nat Rev Mol Cell Biol. 2011; 12:222–234. [PubMed: 21427764]
4. Avasthi P, Marshall WF. Stages of ciliogenesis and regulation of ciliary length. Differentiation. 2012; 83:S30–42. [PubMed: 22178116]
5. Pedersen LB, Veland IR, Schroder JM, Christensen ST. Assembly of primary cilia. Dev Dyn. 2008; 237:1993–2006. [PubMed: 18393310]
6. Hildebrandt F, Benzing T, Katsanis N. Ciliopathies. N Engl J Med. 2011; 364:1533–1543. [PubMed: 21506742]
7. Bettencourt-Dias M, Hildebrandt F, Pellman D, Woods G, Godinho SA. Centrosomes and cilia in human disease. Trends Genet. 2011; 27:307–315. [PubMed: 21680046]
8. Sayer JA, Otto EA, O'Toole JF, Nurnberg G, Kennedy MA, Becker C, Hennies HC, Helou J, Attanasio M, Fausett BV, et al. The centrosomal protein nephrocystin-6 is mutated in Joubert syndrome and activates transcription factor ATF4. Nat Genet. 2006; 38:674–681. [PubMed: 16682973]
9. Coppieters F, Lefever S, Leroy BP, De Baere E. CEP290, a gene with many faces: mutation overview and presentation of CEP290base. Hum Mutat. 2010; 31:1097–1108. [PubMed: 20690115]
10. Valente EM, Silhavy JL, Brancati F, Barrano G, Krishnaswami SR, Castori M, Lancaster MA, Boltshauser E, Boccone L, Al-Gazali L, et al. Mutations in CEP290, which encodes a centrosomal protein, cause pleiotropic forms of Joubert syndrome. Nat Genet. 2006; 38:623–625. [PubMed: 16682970]
11. Kim J, Krishnaswami SR, Gleeson JG. CEP290 interacts with the centriolar satellite component PCM-1 and is required for Rab8 localization to the primary cilium. Hum Mol Genet. 2008; 17:3796–3805. [PubMed: 18772192]
12. Tsang WY, Bossard C, Khanna H, Peranen J, Swaroop A, Malhotra V, Dynlacht BD. CP110 suppresses primary cilia formation through its interaction with CEP290, a protein deficient in human ciliary disease. Dev Cell. 2008; 15:187–197. [PubMed: 18694559]
13. Graser S, Stierhof YD, Lavoie SB, Gassner OS, Lamla S, Le Clech M, Nigg EA. Cep164, a novel centriole appendage protein required for primary cilium formation. J Cell Biol. 2007; 179:321–330. [PubMed: 17954613]
14. Spektor A, Tsang WY, Khoo D, Dynlacht BD. Cep97 and CP110 suppress a cilia assembly program. Cell. 2007; 130:678–690. [PubMed: 17719545]
15. Otto EA, Loeys B, Khanna H, Hellemans J, Sudbrak R, Fan S, Muerb U, O'Toole JF, Helou J, Attanasio M, et al. Nephrocystin-5, a ciliary IQ domain protein, is mutated in Senior-Loken syndrome and interacts with RPGR and calmodulin. Nat Genet. 2005; 37:282–288. [PubMed: 15723066]
16. Otto EA, Helou J, Allen SJ, O'Toole JF, Wise EL, Ashraf S, Attanasio M, Zhou W, Wolf MT, Hildebrandt F. Mutation analysis in nephronophthisis using a combined approach of homozygosity mapping, CEL I endonuclease cleavage, and direct sequencing. Hum Mutat. 2008; 29:418–426. [PubMed: 18076122]
17. Stone EM, Cideciyan AV, Aleman TS, Scheetz TE, Sumaroka A, Ehlinger MA, Schwartz SB, Fishman GA, Traboulsi EI, Lam BL, et al. Variations in NPHP5 in patients with nonsyndromic leber congenital amaurosis and Senior-Loken syndrome. Arch Ophthalmol. 2011; 129:81–87. [PubMed: 21220633]
18. Estrada-Cuzcano A, Koenekoop RK, Coppieters F, Kohl S, Lopez I, Collin RW, De Baere EB, Roeleveld D, Marek J, Bernd A, et al. IQCB1 mutations in patients with leber congenital amaurosis. Invest Ophthalmol Vis Sci. 2011; 52:834–839. [PubMed: 20881296]

19. Schafer T, Putz M, Lienkamp S, Ganner A, Bergbreiter A, Ramachandran H, Gieloff V, Gerner M, Mattonet C, Czarnecki PG, et al. Genetic and physical interaction between the NPHP5 and NPHP6 gene products. Hum Mol Genet. 2008; 17:3655–3662. [PubMed: 18723859]
20. Chang B, Khanna H, Hawes N, Jimeno D, He S, Lillo C, Parapuram SK, Cheng H, Scott A, Hurd RE, et al. In-frame deletion in a novel centrosomal/ciliary protein CEP290/NPHP6 perturbs its interaction with RPGR and results in early-onset retinal degeneration in the rd16 mouse. Hum Mol Genet. 2006; 15:1847–1857. [PubMed: 16632484]
21. Sang L, Miller JJ, Corbit KC, Giles RH, Brauer MJ, Otto EA, Baye LM, Wen X, Scales SJ, Kwong M, et al. Mapping the NPHP-JBTS-MKS protein network reveals ciliopathy disease genes and pathways. Cell. 2011; 145:513–528. [PubMed: 21565611]
22. Luo X, He Q, Huang Y, Sheikh MS. Cloning and characterization of a p53 and DNA damage down-regulated gene PIQ that codes for a novel calmodulin-binding IQ motif protein and is up-regulated in gastrointestinal cancers. Cancer Res. 2005; 65:10725–10733. [PubMed: 16322217]
23. Otto EA, Hurd TW, Airik R, Chaki M, Zhou W, Stoetzel C, Patil SB, Levy S, Ghosh AK, Murga-Zamalloa CA, et al. Candidate exome capture identifies mutation of SDCCAG8 as the cause of a retinal-renal ciliopathy. Nat Genet. 2010; 42:840–850. [PubMed: 20835237]
24. Kim J, Lee JE, Heynen-Genel S, Suyama E, Ono K, Lee K, Ideker T, Aza-Blanc P, Gleeson JG. Functional genomic screen for modulators of ciliogenesis and cilium length. Nature. 2010; 464:1048–1051. [PubMed: 20393563]
25. Dawe HR, Smith UM, Cullinane AR, Gerrelli D, Cox P, Badano JL, Blair-Reid S, Sriram N, Katsanis N, Attie-Bitach T, et al. The Meckel-Gruber Syndrome proteins MKS1 and meckelin interact and are required for primary cilium formation. Hum Mol Genet. 2007; 16:173–186. [PubMed: 17185389]
26. Chaki M, Hoefele J, Allen SJ, Ramaswami G, Janssen S, Bergmann C, Heckenlively JR, Otto EA, Hildebrandt F. Genotype-phenotype correlation in 440 patients with NPHP-related ciliopathies. Kidney Int. 2011; 80:1239–1245. [PubMed: 21866095]
27. Wang X, Wang H, Cao M, Li Z, Chen X, Patenia C, Gore A, Abboud EB, Al-Rajhi AA, Lewis RA, et al. Whole-exome sequencing identifies ALMS1, IQCB1, CNGA3, and MYO7A mutations in patients with Leber congenital amaurosis. Hum Mutat. 2011; 32:1450–1459. [PubMed: 21901789]
28. Otto EA, Ramaswami G, Janssen S, Chaki M, Allen SJ, Zhou W, Airik R, Hurd TW, Ghosh AK, Wolf MT, et al. Mutation analysis of nephronophthisis associated ciliopathy disease genes using a DNA pooling and next generation sequencing strategy. J Med Genet. 2011; 48:105–116. [PubMed: 21068128]
29. Fahim AT, Bowne SJ, Sullivan LS, Webb KD, Williams JT, Wheaton DK, Birch DG, Daiger SP. Allelic heterogeneity and genetic modifier loci contribute to clinical variation in males with X-linked retinitis pigmentosa due to RPGR mutations. PLoS One. 2011; 6:e23021. [PubMed: 21857984]
30. Kobayashi T, Tsang WY, Li J, Lane W, Dynlacht BD. Centriolar kinesin Kif24 interacts with CP110 to remodel microtubules and regulate ciliogenesis. Cell. 2011; 145:914–925. [PubMed: 21620453]
31. Gakovic M, Shu X, Kasioulis I, Carpanini S, Moraga I, Wright AF. The role of RPGR in cilia formation and actin stability. Hum Mol Genet. 2011; 20:4840–4850. [PubMed: 21933838]
32. Stowe TR, Wilkinson CJ, Iqbal A, Stearns T. The centriolar satellite proteins Cep72 and Cep290 interact and are required for recruitment of BBS proteins to the cilium. Mol Biol Cell. 2012; 23:3322–3335. [PubMed: 22767577]
33. Lopes CA, Prosser SL, Romio L, Hirst RA, O'Callaghan C, Woolf AS, Fry AM. Centriolar satellites are assembly points for proteins implicated in human ciliopathies, including oral-facial-digital syndrome 1. J Cell Sci. 2011; 124:600–612. [PubMed: 21266464]
34. Singla V, Romaguera-Ros M, Garcia-Verdugo JM, Reiter JF. Ofd1, a human disease gene, regulates the length and distal structure of centrioles. Dev Cell. 2010; 18:410–424. [PubMed: 20230748]
35. Hard T, Lendel C. Inhibition of amyloid formation. J Mol Biol. 2012; 421:441–465. [PubMed: 22244855]

36. Wakatsuki T, Schwab B, Thompson NC, Elson EL. Effects of cytochalasin D and latrunculin B on mechanical properties of cells. J Cell Sci. 2001; 114:1025–1036. [PubMed: 11181185]

37. Schultze A, Fiedler W. Therapeutic potential and limitations of new FAK inhibitors in the treatment of cancer. Expert Opin Investig Drugs. 2010; 19:777–788.

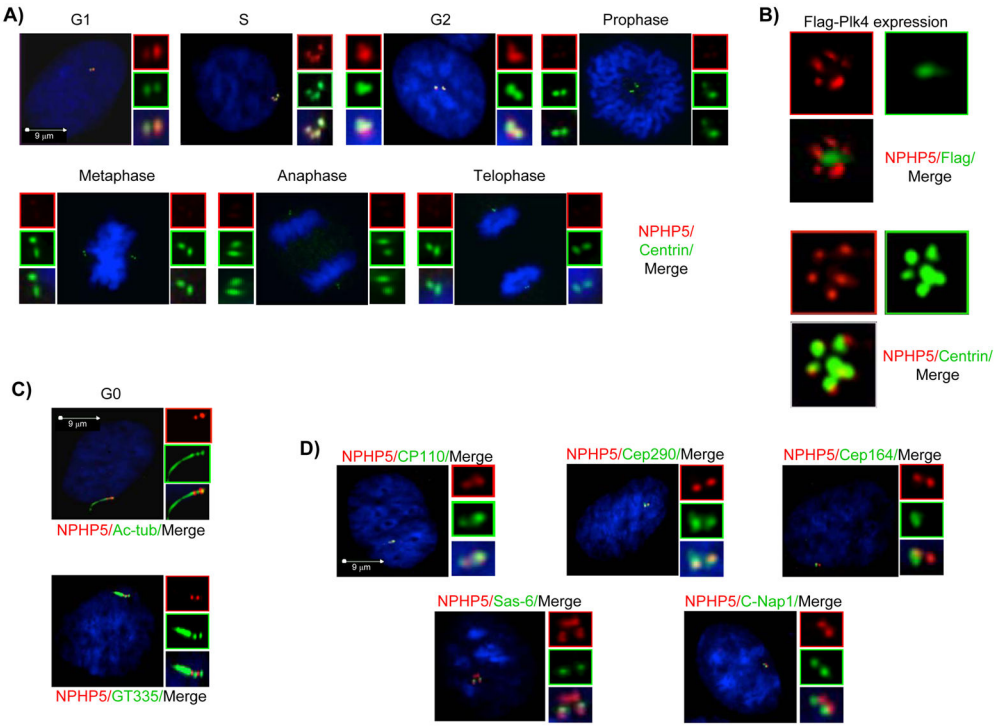

Figure 1.

NPHP5 localizes to the distal region of centrioles and is cell cycle regulated. (**A**) RPE-1 cells in different stages of the cell cycle were processed for immunofluorescence with anti-NPHP5 (red) and anti-centrin (green) antibodies. DNA was stained with DAPI (blue). (**B**) U2OS cells transiently transfected with plasmid expressing Flag-Plk4 to induce simultaneous production of multiple procentrioles adjoining a single parental centriole were stained with antibodies against NPHP5 (red) and Flag or centrin (green). (**C**) Quiescent RPE-1 cells were processed for immunofluorescence with anti-NPHP5 (red) and anti-glutamylated tubulin (GT335) or anti-acetylated tubulin (Ac-tub) (green) antibodies. DNA was stained with DAPI (blue). (**D**) RPE-1 cells were processed for immunofluorescence with anti-NPHP5 (red) and anti-CP110, anti-Cep290, anti-Cep164, anti-Sas-6 or anti-C-Nap-1 (green) antibodies. DNA was stained with DAPI (blue).

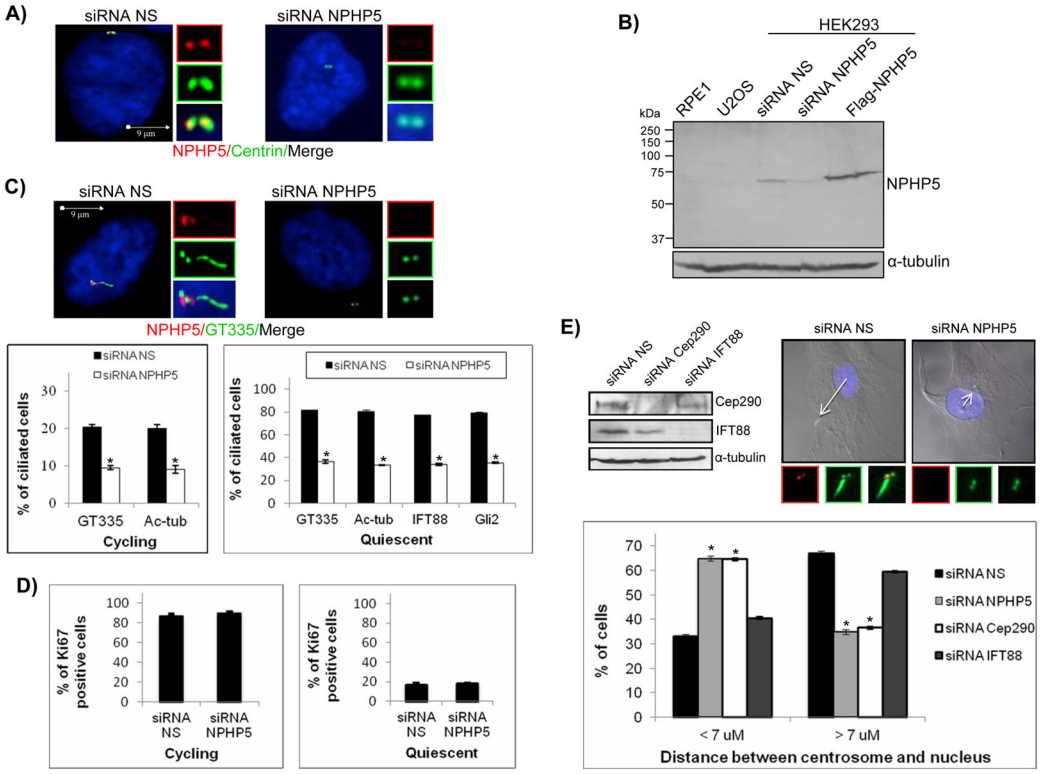

Figure 2.

RNAi-mediated suppression of NPHP5 inhibits an early step of cilia formation. (**A**) RPE-1 cells were transfected with control (NS) or NPHP5 siRNAs and processed for immunofluorescence with anti-NPHP5 (red) and anti-centrin (green) antibodies. DNA was stained with DAPI (blue). (**B**) Extracts from RPE-1, U2OS or HEK293 cells transfected with control (NS) or NPHP5 siRNAs, or transfected with plasmid expressing full-length Flag-NPHP5 were probed by Western blotting with anti-NPHP5 antibody. α-tubulin was used as a loading control. (**C**) RPE-1 cells transfected with control (NS) or NPHP5 siRNAs, induced to quiescence, and stained with antibodies against NPHP5 (red) and glutamylated tubulin (GT335), and with DAPI (blue) (pictures). The percentages of cycling (left graph) and quiescent (right graph) RPE-1 cells with primary cilia were determined using glutamylated tubulin (GT335), acetylated tubulin (Ac-tub), IFT88 or Gli2 as ciliary markers. (**D**) The percentages of cycling (left graph) and quiescent (right graph) RPE-1 cells stained positive for the proliferative marker Ki67 were determined. (**E**) RPE-1 cells transfected with control (NS) or NPHP5 siRNAs, induced to quiescence, and stained with antibodies against NPHP5 (red) and glutamylated tubulin (GT335, green), and with DAPI (blue). Fluorescent images were merged with corresponding differential interference contrast images. The distance from the center of the nucleus to the centrosome was measured and indicated by a white arrowed line (pictures). The percentages of control (NS), NPHP5, Cep290 or IFT88 siRNA-treated quiescent RPE-1 cells having a nucleus-to-centrosome distance of <7 μm and >7 μm were determined (graph). In (**C-E**), the average of 2–3 independent experiments is shown. Error bars represent standard errors. At least 100 cells for each siRNA condition were scored each time. *p<0.01 compared with NS.

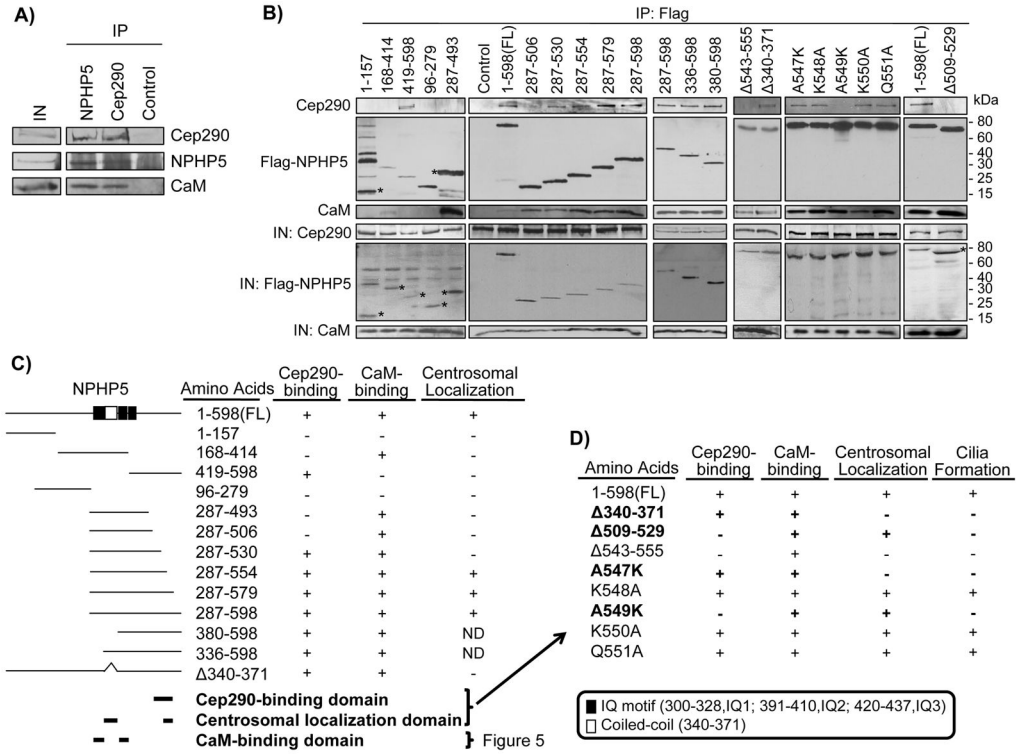

Figure 3.

NPHP5 interacts with Cep290 and CaM and possesses distinct functional domains. (**A**) Western blotting of endogenous Cep290, NPHP5 and CaM after immunoprecipitation from HEK293 extracts with anti-NPHP5, anti-Cep290 or anti-Flag (control) antibodies. IN denotes input. (**B**) Flag (control), full-length (FL) or the indicated fragments and mutants of Flag-tagged NPHP5 were expressed in HEK293 cells and immunoprecipitated from lysates. Flag-NPHP5, Cep290 and CaM were detected after western blotting the resulting immunoprecipitates. IN indicates input. An asterisk denotes a band corresponding to the expected recombinant protein. (**C–D**) Summary of the results of *in vivo* binding, centrosomal localization and cilia rescue experiments using NPHP5 truncation, deletion and single-point mutants. FL, Δ and ND denote full-length, deletion and not determined, respectively. A putative coiled coil domain is located at amino acid residues 340-371, while three putative IQ CaM-binding motifs reside at residues 300-328, 391-410 and 420-437. Further mapping results are shown in Figure 5.

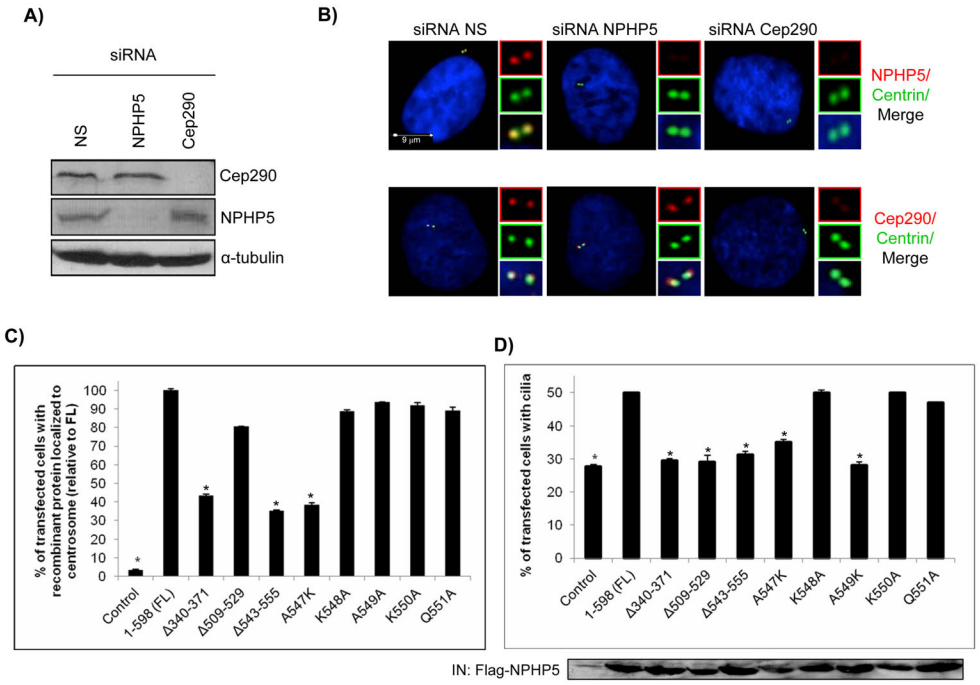

Figure 4.

NPHP5 interaction with Cep290 is crucial for cilia formation. (**A**) Western blotting of Cep290 and NPHP5 in HEK293 cells treated with control (NS), NPHP5 or Cep290 siRNAs. α-tubulin was used as a loading control. (**B**) RPE-1 cells transfected with control (NS), NPHP5 or Cep290 siRNAs were stained with antibodies against NPHP5 or Cep290 (red) and centrin (green), and with DAPI (blue). Identical results were also obtained in HEK293 cells. (**C**) The percentages of transfected, cycling RPE-1 cells showing proper recombinant protein localization to centrosomes, relative to full-length, were determined using centrin as a centrosomal marker. Control denotes expression of an irrelevant Flag-tagged protein. FL denotes full-length. (**D**) The percentages of transfected, quiescent and NPHP5 siRNA-depleted ARPE-19 cells expressing primary cilia were determined using acetylated tubulin as a marker. Note that NPHP5 siRNA oligo 5 was used. Control denotes expression of an irrelevant Flag-tagged protein. FL denotes full-length. In (**C–D**), at least 75 transfected cells were scored for each construct, and average data obtained from three independent experiments is shown. Error bars represent standard errors. *$p<0.01$ compared with FL.

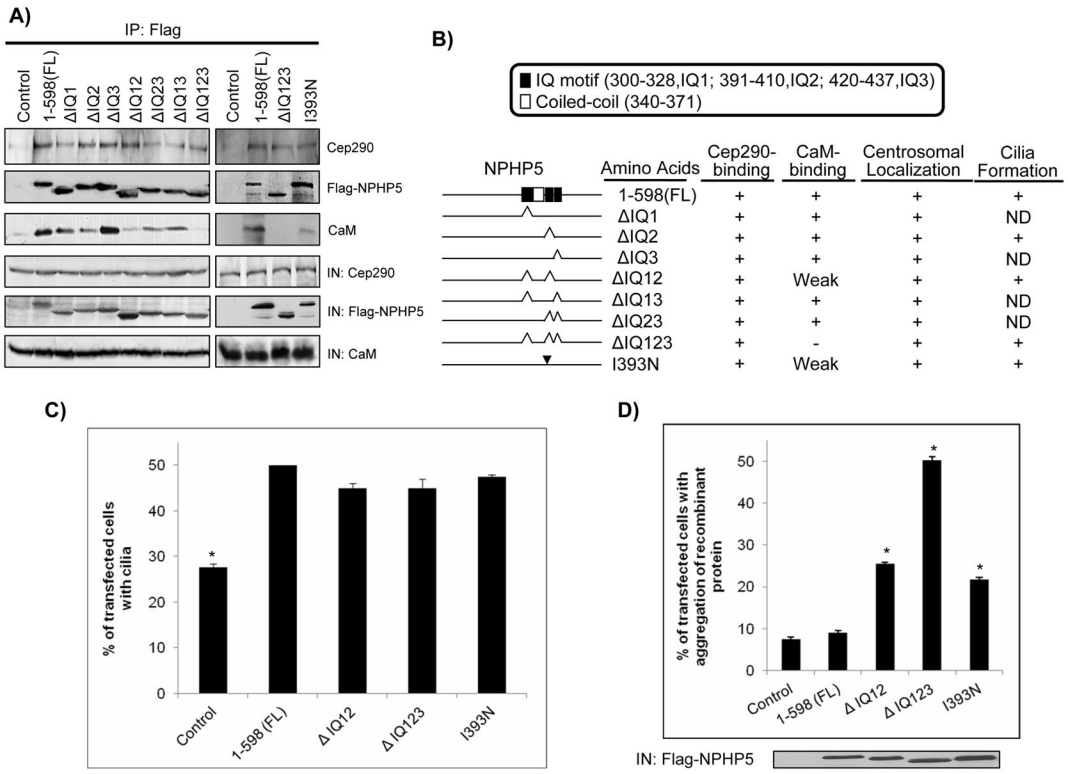

Figure 5.

NPHP5 interaction with CaM prevents aggregate formation. (**A**) Flag (control), full-length (FL) or the indicated mutants of Flag-tagged NPHP5 were expressed in HEK293 cells and immunoprecipitated from lysates. Flag-NPHP5, Cep290 and CaM were detected after western blotting the resulting immunoprecipitates. IN indicates input. (**B**) Summary of the results of *in vivo* binding, centrosomal localization and cilia rescue experiments using NPHP5 truncation, deletion and single-point mutants. FL, Δ and ND denote full-length, deletion and not determined, respectively. (**C**) The percentages of transfected, quiescent and NPHP5 siRNA-depleted ARPE-19 cells expressing primary cilia were determined using acetylated tubulin as a marker. Note that NPHP5 siRNA oligo 5 was used. Control denotes expression of an irrelevant Flag-tagged protein. FL denotes full-length. (**D**) The percentages of transfected, cycling RPE-1 cells possessing recombinant protein aggregates were determined using Flag as a marker. Control denotes expression of an irrelevant Flag-tagged protein. FL denotes full-length. In (**C–D**), at least 75 transfected cells were scored for each construct, and average data obtained from three independent experiments is shown. Error bars represent standard errors. *p<0.01 compared with FL.

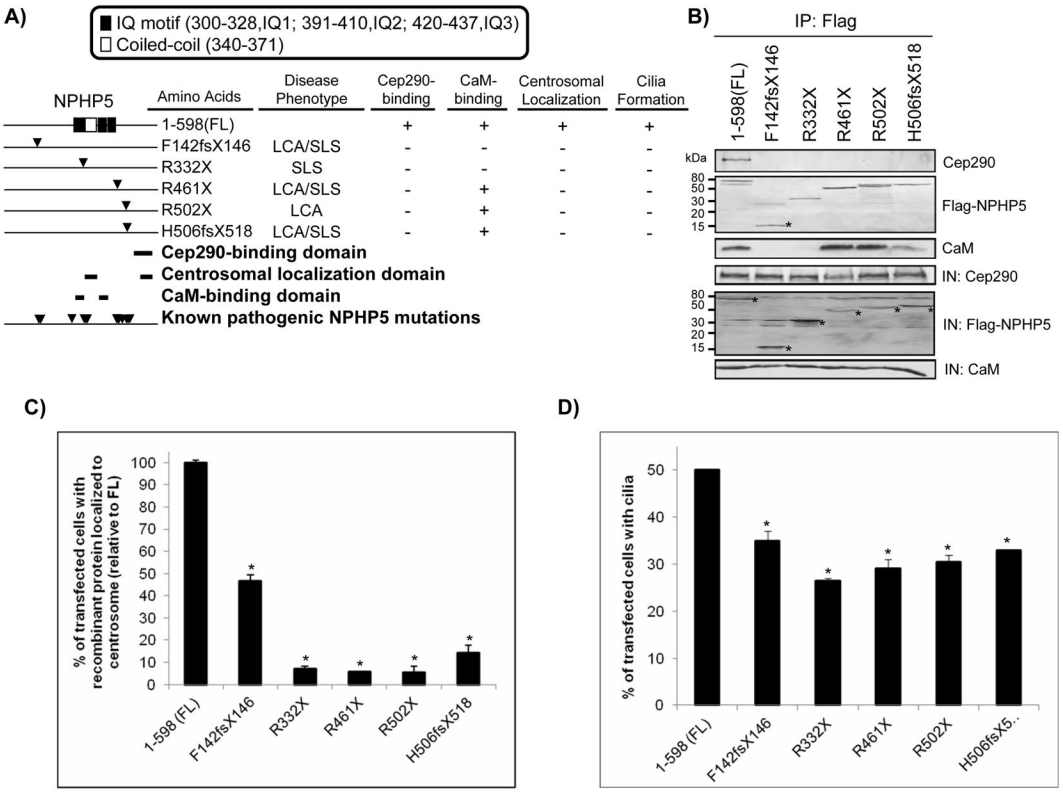

Figure 6.

Pathogenic *NPHP5* mutations abolish protein interaction with Cep290, induce protein mis-localization and inhibit cilia formation. (**A**) Summary of the results of *in vivo* binding, centrosomal localization and cilia rescue experiments using NPHP5 disease-causing mutants. FL, fs and X denote full-length, frameshift and termination, respectively. Known pathogenic mutations causing SLS and LCA are indicated by inverted triangles. Disease phenotypes associated with F142fsX146, R332X, R461X, R502X and H506fsX518 mutations are indicated. (**B**) Full-length (FL) or the indicated mutants of Flag-tagged NPHP5 were expressed in HEK293 cells and immunoprecipitated from lysates. Flag-NPHP5, Cep290 and CaM were detected after western blotting the resulting immunoprecipitates. IN indicates input. An asterisk denotes a band corresponding to the expected recombinant protein. (**C**) The percentages of transfected, cycling RPE-1 cells showing proper recombinant protein localization to centrosomes, relative to full-length, were determined using centrin as a centrosomal marker. FL denotes full-length. (**D**) The percentages of transfected, quiescent and NPHP5 siRNA-depleted ARPE-19 cells expressing primary cilia were determined using acetylated tubulin as a marker. Note that NPHP5 siRNA oligo 5 was used. FL denotes full-length. In (**C–D**), at least 75 transfected cells were scored for each construct, and average data obtained from three independent experiments is shown. Error bars represent standard errors. *$p<0.01$ compared with FL.

A)

Protein	Function	Drug
CP110	Distal end capping of centriolar microtubules	Not available
FAK	Focal adhesion assembly	PF573228 (PF)
		FAK inhibitor 14 (FAK I)
ACTIN	Cytoskeleton Formation	Cytochalasin D (CytoD)
		Latrunculin B (LatB)
ARP3	Branched Actin polymerization	CK548
		CK636
PLA2G3	Membrane trafficking	OPC
		CAY10590 (CAY)
XIAP	Apoptosis regulation	TPEN
		Embelin

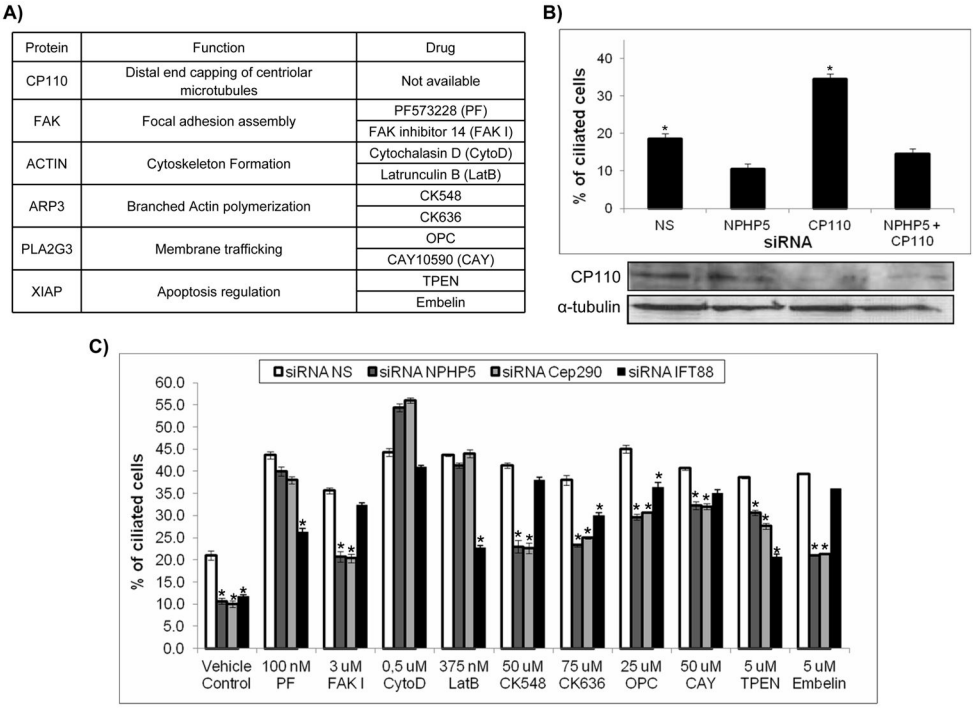

Figure 7.

Inhibition of negative regulators of the ciliogenic pathway restores cilia formation in the absence of NPHP5. (**A**) A table summarizing proteins known to inhibit ciliogenesis and their corresponding biological functions, along with drugs known to target these proteins. (**B**) The percentages of control (NS), NPHP5, CP110 or double siRNA-treated cycling RPE-1 cells with primary cilia were determined using glutamylated tubulin as a marker. (**C**) The percentages of control (NS), NPHP5, Cep290 or IFT88 siRNA-treated cycling RPE-1 cells exposed to drugs and possessing primary cilia were determined using glutamylated tubulin as a marker. In (**B–C**), at least 75 transfected cells were scored for each siRNA condition, and average data obtained from three independent experiments is shown. Error bars represent standard errors. In (**B**), *p<0.01 compared with NPHP5 knockdown. In (**C**), *p<0.01 compared with NS.